Hot QCD equations of state and relativistic heavy ion collisions

Vinod Chandra* and Ravindra Kumar†
Department of Physics, IIT Kanpur, Kanpur 208 016, India

V. Ravishankar‡
Department of Physics, IIT Kanpur, Kanpur 208 016, India, and Raman Research Institute, Bangalore 560 080, India

(Received 16 July 2007; revised manuscript received 19 September 2007; published 28 November 2007; corrected 3 December 2007)

We study two recently proposed equations of state obtained from high-temperature QCD and show how they can be adapted to use them for making predictions for relativistic heavy ion collisions. The method involves extracting equilibrium distribution functions for quarks and gluons from the equation of state (EOS), which in turn will allow a determination of the transport and other bulk properties of the quark gluon-plasma. Simultaneously, the method also yields a quasiparticle description of interacting quarks and gluons. The first EOS is perturbative in the QCD coupling constant and has contributions of $O(g^5)$. The second EOS is an improvement over the first, with contributions up to $O[g^6 \ln(1/g)]$; it incorporates the nonperturbative hard thermal contributions. The interaction effects are shown to be captured entirely by the effective chemical potentials for the gluons and the quarks, in both cases. The chemical potential is seen to be highly sensitive to the EOS. As an application, we determine the screening lengths, which are, indeed, the most important diagnostics for QGP. The screening lengths are seen to behave drastically differently depending on the EOS considered and therefore yield a way to distinguish the two equations of state in heavy ion collisions.

DOI: 10.1103/PhysRevC.76.054909 PACS number(s): 25.75.−q, 24.85.+p, 12.38.Mh, 21.65.+f

I. INTRODUCTION

Recent experimental results [1–4] indicate that the quark-gluon plasma (QGP) has already been produced at RHIC and that its behavior is not close to that of an ideal gas. Indeed, measurements of flow parameters [1] and observations of jet quenching [5] have stimulated the theoretical interpretation that the QGP behaves like a nearly perfect fluid [6], characterized by a small value of the viscosity to entropy density ratio, lying in the range 0.1–0.3 [7–9]; this range may be contrasted with the corresponding value for liquid helium (above superfluid transition temperature), which is close to 10 [10]. These observations signal the fact that the deconfined phase is strongly interacting and are consistent with the lattice simulations [11], which predict a strongly interacting behavior even at temperatures of a few times the critical temperature T_c. In an attempt to appreciate this surprising result, interesting analogies have been drawn with AdS/CFT correspondence [10] and also with some strongly coupled classical systems [12]. In any case, the emergence of the strongly interacting behavior puts into doubt the credibility of a large body of analyses that are based on ideal or nearly ideal behavior of QGP.

In this context, there is an interesting attempt by Arnold and Zhai [13] and Zhai and Kastening [14], who have determined the equation of state (EOS) of interacting quarks and gluons up to $O(g^5)$ in the coupling constant. This strictly perturbative EOS, which we henceforth denote by EOS1, has been improved upon by Kajantie *et al.* [15,16], who have incorporated the contributions from the nonperturbative scales (i.e., gT and g^2T) and determined the EOS up to $O[g^6 \ln(1/g)]$ [17]. The latter will be denoted by EOS2. Subsequent studies [18–20] have emphasized the relevance of these equations of state for studying QGP. One would naturally wish to compare these equations of state with (the fully nonperturbative) lattice results. EOS2 has been found [15] to be in qualitative agreement with the lattice results. It is not without interest to explore further whether this qualitative agreement can be further quantified, and whether a hard thermal loop (HTL) improved EOS can describe the QGP produced in heavy ion collisions. It is worthwhile noting the earlier attempts [21–23] that have been made to determine thermodynamic quantities such as entropy and the specific heat c_v in improved perturbative approaches to QGP.

On the other hand, it is by now well established that the semiclassical approach is a convenient way to study the bulk properties of QGP [24–28], since they automatically incorporate the HTL effects [27,28]. There is a wealth of results that have been obtained within this framework [24–26], where the nonperturbative features manifest as effective mean color fields. These color fields have the dual role of producing the soft and semisoft partons, apart from modulating their interactions. The emergence of such effective field degrees of freedom, together with a classical transport, has been indicated earlier by Blaizot and Iancu [29].

In this context, it is pertinent to ask whether one could use heavy ion collisions to distinguish the various equations of state and pick the right one, by employing the semiclassical framework involving an appropriate kinetic equation. The purpose of this paper is to explore such possibilities. As a first step in this direction, we shall show how the distribution functions underlying the proposed EOS can be extracted with a minimal ansatz (i.e., the effective chemical potentials for

*vinodc@iitk.ac.in
†rojha@iitk.ac.in
‡vravi@iitk.ac.in

quarks and gluons). Once the distribution function is obtained, it can be used to study the bulk properties of the system such as chromo responses, including the ubiquitous Debye mass. Postponing all the other applications to a future work, we shall concentrate on determining the Debye mass through this procedure. As mentioned, we focus on EOS1 and EOS2. Both of these have been proposed for the case when the baryon number density vanishes. The corresponding chemical potentials are hence set to zero. There exist generalizations of these equations of state, proposed by Vuorinen [30] and more recently by Ipp *et al*. [17] (who have determined the equations of state up to order g^4 at all chemical potentials and also claim the validity of their equations of state for all temperatures), which allow for a finite baryon number. The two sets are applicable to distinct physical situations; the former (EOS1 and EOS2) are relevant to the QGP in the central midrapidity region of URHIC whereas the works of Refs. [17,30] are applicable to peripheral collisions and/or when the so-called nuclear transparency is only partial. An application of these equations of state to URHIC will be taken up separately.

This paper is organized as follows. In the next section, we extract the distribution functions for the gluons and the quarks from EOS1 and EOS2. We consider the pure gluonic case separately from the full QCD, by first setting $N_f = 0$. The (interacting) quark sector is then dealt with. In Sec. III, the Debye mass is determined by employing the semiclassical method developed by Kelly *et al*. [27,28]. In Sec. III(B), we compare our results on screening length for EOS1 and EOS2 with the recent lattice results. We summarize the results and conclude in Sec. IV. The Appendix contains some details of calculations that are not explicitly given in the main text; it also lists some useful integrals.

II. EXTRACTION OF THE DISTRIBUTION FUNCTIONS

Recently, Arnold *et al*. [13] have derived an equation of state (EOS1) for high-temperature QCD up to $O(g^5)$. EOS1 reads

$$\begin{aligned} P^{(1)} = {} & \frac{8\pi^2}{45\beta^4}\left\{\left(1+\frac{21N_f}{32}\right)-\frac{15}{4}\left(1+\frac{5N_f}{12}\right)\frac{\alpha_s}{\pi}\right. \\ & +30\left(1+\frac{N_f}{6}\right)\left(\frac{\alpha_s}{\pi}\right)^{\frac{3}{2}} \\ & +\left[237.2+15.97N_f-0.413N_f^2\right. \\ & +\frac{135}{2}\left(1+\frac{N_f}{6}\right)\ln\left(\frac{\alpha_s}{\pi}(1+N_f/6)\right) \\ & \left.-\frac{165}{8}\left(1+\frac{5N_f}{12}\right)\left(1-\frac{2N_f}{33}\right)\ln\left(\frac{\bar{\mu}_{\rm MS}\beta}{2\pi}\right)\right]\left(\frac{\alpha_s}{\pi}\right)^2 \\ & +\left(1+\frac{N_f}{6}\right)^{\frac{1}{2}}\left[-799.2-21.99N_f-1.926N_f^2\right. \\ & \left.\left.+\frac{495}{2}\left(1+\frac{N_f}{6}\right)\left(1+\frac{2N_f}{33}\right)\ln\left(\frac{\bar{\mu}_{\rm MS}\beta}{2\pi}\right)\right]\left(\frac{\alpha_s}{\pi}\right)^{\frac{5}{2}}\right\} \\ & +O(\alpha_s)^3\ln(\alpha_s). \end{aligned} \tag{1}$$

EOS1 has been subsequently improved by Kajantie *et al*. [15,16], who proposed another equation of state (EOS2) by improving the accuracy to the next order in the coupling constant. They also included the HTL effects(which are essentially nonperturbative and contain contributions from scales T, gT, andg^2T). EOS2, which is thus determined up to $O[g^6\ln(1/g)]$, has the form

$$\begin{aligned} P^{(2)} = {} & P^{(1)}+\frac{8\pi^2}{45}T^4\left[1134.8+65.89N_f+7.653N_f^2\right. \\ & \left.-\frac{1485}{2}\left(1+\frac{1}{6}N_f\right)\left(1-\frac{2}{33}N_f\right)\ln\left(\frac{\bar{\mu}_{\rm MS}}{2\pi T}\right)\right] \\ & \times\left(\frac{\alpha_s}{\pi}\right)^3\ln\frac{1}{\alpha_s}. \end{aligned} \tag{2}$$

In these expressions, N_f is the number of fermions, $\alpha_s = g^2/(4\pi)$ is the strong coupling constant, and $\bar{\mu}_{\rm MS}$ is the renormalization scale parameter in the $\overline{\rm MS}$ scheme. Note that α_s runs with β and $\bar{\mu}_{\rm MS}$. As remarked, the utility of this EOS in the context of QGP thermodynamics has been discussed earlier by Rebhan [20].

We now set to determine equilibrium distribution functions $\langle n_{g,f}\rangle$ for the gluons and the quarks such that they would yield these particular equations of state. The ansatz for the determination involves retaining the ideal distribution forms, with the chemical potentials μ_g and μ_f being free parameters. Note that for the massless quarks (u and d), which we consider to constitute the bulk of the plasma, $\mu \equiv 0$ if they were not interacting. This approach is of course not novel, since it underlies many of the ideas whose aim is to describe the interaction effects in terms of the quasiparticle degrees of freedom. In the present context, we refer the reader to Refs. [31,32], where an attempt is made to describe the lattice results in terms of effective mass for the partons.

We pause to note that the chemical potentials that we introduce are not the same as those that yield a nonzero baryon number density, as, for example, in Refs. [17,30]. Here, the chemical potential merely serves to map the interacting quarks and gluons at zero baryon number chemical potential to noninteracting quasiparicles (i.e., the dressed quarks and gluons). Their interpretation is, therefore, more akin to the effective mass, albeit as functions of the renormalization scale and temperature as we show in the following. Thus, the baryon number density of the plasma continues to vanish.

As the first step in our approach, we express the EOS in the form

$$P = P_g^I + P_q^I + \Delta P_g + \Delta P_f. \tag{3}$$

The first two terms in the right-hand side of Eq. (3) are identified with the distributions of an ideal gas of quarks and gluons. The effects of the interaction in pure QCD are represented by ΔP_g and the residual interaction effects by ΔP_f. For the EOS in which we are interested, the identification of these terms is straightforward. ΔP_g can be identified by first setting $N_f = 0$ and then subtracting the ideal part. The residual term is naturally identified as ΔP_f after the ideal part for quarks is subtracted. The general form of the EOS [see

Eq. (1) and Eq. (2)] is

$$P = \frac{8\pi^2}{45}\beta^{-4}\left[1 + A(\alpha_s) + B(\alpha_s)\ln\frac{\bar{\mu}_{\rm MS}\beta}{2\pi} + \frac{21}{32}N_f + C(\alpha_s, N_f) + D(\alpha_s, N_f)\ln\frac{\bar{\mu}_{\rm MS}\beta}{2\pi}\right], \quad (4)$$

where

$$\begin{aligned} P_g^I &= \frac{8\pi^2}{45}\beta^{-4}, \\ P_f^I &= \frac{8\pi^2}{45}\beta^{-4}\frac{21}{32}N_f, \\ \Delta P_g &= A(\alpha_s) + B(\alpha_s)\ln\frac{\bar{\mu}_{\rm MS}\beta}{2\pi}, \\ \Delta P_f &= C(\alpha_s, N_f) + D(\alpha_s, N_f)\ln\frac{\bar{\mu}_{\rm MS}\beta}{2\pi}. \end{aligned} \quad (5)$$

For EOS1 the coefficients A, B, C, and D are denoted with a prime and are given by

$$\begin{aligned} A'[\alpha_s(N_f)] &= -\frac{15}{4}\frac{\alpha_s}{\pi} + 30\left(\frac{\alpha_s}{\pi}\right)^{\frac{3}{2}} + \left[237.2 + \frac{135}{2}\log\left(\frac{\alpha_s}{\pi}\right)\right]\left(\frac{\alpha_s}{\pi}\right)^2 - 799.2\left(\frac{\alpha_s}{\pi}\right)^{\frac{5}{2}}, \\ B'[\alpha_s(N_f)] &= -\frac{165}{8}\left(\frac{\alpha_s}{\pi}\right)^2 + \frac{495}{2}\left(\frac{\alpha_s}{\pi}\right)^{\frac{5}{2}}, \\ C'[\alpha_s(N_f), N_f] &= -\frac{15}{4}\left(1 + \frac{5}{12}N_f\right)\frac{\alpha_s}{\pi} + 30\left(1 + \frac{1}{6}N_f\right)\left(\frac{\alpha_s}{\pi}\right)^{\frac{3}{2}} + \left[237.2 + 15.97N_f - 0.413N_f^2 + \frac{135}{2}\right. \\ &\quad \left.\times\left(1 + \frac{N_f}{6}\right)\ln\left[\frac{\alpha_s}{\pi}(1 + N_f/6)\right]\right]\left(\frac{\alpha_s}{\pi}\right)^2 + (1 + N_f/6)^{1/2}\left[-799.2 - 21.99N_f - 1.926N_f^2\right]\left(\frac{\alpha_s}{\pi}\right)^{\frac{5}{2}} - A'[\alpha_s(N_f)], \\ D'[\alpha_s(N_f), N_f] &= -\frac{165}{8}\left(1 + \frac{5}{12}N_f\right)\left(1 - \frac{2}{33}N_f\right)\left(\frac{\alpha_s}{\pi}\right)^2 + \frac{495}{2}\left(1 + \frac{1}{6}N_f\right)\left(1 - \frac{2}{33}\right)\left(\frac{\alpha_s}{\pi}\right)^{\frac{5}{2}} - B'[\alpha_s(N_f)], \end{aligned} \quad (6)$$

whereas for EOS2 the coefficients can be written in terms of the these primed coefficients for EOS1 as

$$\begin{aligned} A[\alpha_s(N_f)] &= A'[\alpha_s(N_f)] + 1134.8\left(\frac{\alpha_s}{\pi}\right)^3\log\left(\frac{1}{\alpha_s}\right), \\ B[\alpha_s(N_f)] &= B'[\alpha_s(N_f)] - \frac{1485}{2}\left(\frac{\alpha_s}{\pi}\right)^3\log\left(\frac{1}{\alpha_s}\right), \\ C[\alpha_s(N_f), N_f] &= C'[\alpha_s(N_f), N_f] + \left(65.89N_f + 7.653N_f^2\right)\times\left(\frac{\alpha_s}{\pi}\right)^3\log\left(\frac{1}{\alpha_s}\right), \\ D[\alpha_s(N_f), N_f] &= D'[\alpha_s(N_f), N_f] - \frac{1485}{2}\left[\left(1 + \frac{1}{6}N_f\right)\left(1 - \frac{2}{33}N_f\right) - 1\right]\times\left(\frac{\alpha_s}{\pi}\right)^3\log\left(\frac{1}{\alpha_s}\right). \end{aligned} \quad (7)$$

We seek to parametrize the contributions from all the nonideal coefficients in terms the chemical potentials μ_g and μ_f for gluons and quarks, respectively. Because the equations of state have been proposed at high T, with their validity being at temperatures greater than $2T_c$ [33], we treat the dimensionless quantity $\tilde{\mu}_{g,f} \equiv \beta\mu_{g,f}$ perturbatively. This approximation needs to be implemented self-consistently, and accordingly, we expand the grand canonical partition functions for gluons and quarks as a Taylor series in $\tilde{\mu}_{g,f}$. We obtain the following expressions:

$$\begin{aligned} \log(Z_g) &= \sum_{k=0}^{\infty}(\tilde{\mu}_g)^k\partial_{\tilde{\mu}_g}^k\log(Z_g)|_{(\tilde{\mu}_g=0)}, \\ \log(Z_q) &= \sum_{k=0}^{\infty}(\tilde{\mu}_f)^k\partial_{\tilde{\mu}_f}^k\log(Z_f)|_{(\tilde{\mu}_f=0)}, \end{aligned} \quad (8)$$

where Z_g and Z_f are given by

$$\begin{aligned} Z_g &= \prod_p \frac{1}{[1 - \exp(-\beta\epsilon_p + \tilde{\mu}_g)]}, \\ Z_q &= \prod_p [1 + \exp(-\beta\epsilon_p + \tilde{\mu}_f)]. \end{aligned} \quad (9)$$

We determine Z_g and Z_q [defined in Eq. (8)] up to $O(\tilde{\mu}_{g,f})^3$. The truncation is seen to yield an accuracy of $\sim$10% when we consider EOS1. However, for the more physical EOS2, the agreement is within 1%. The gluon chemical potential μ_g gets determined by

$$\frac{A_g^{(3)}}{3!}(\tilde{\mu}_g)^3 + \frac{A_g^{(2)}}{2!}(\tilde{\mu}_g)^2 + A_g^{(1)}\tilde{\mu}_g - \Delta P_g\beta V = 0. \quad (10)$$

Similarly, the equation determining μ_f reads

$$\frac{A_f^{(3)}}{3!}(\tilde{\mu}_f)^3 + \frac{A_f^{(2)}}{2!}(\tilde{\mu}_f)^2 + A_f^{(1)}\tilde{\mu}_f - \Delta P_f\beta V = 0. \quad (11)$$

The coefficients $A_g^{(n)}$ and $A_f^{(n)}$ are given by

$$\begin{aligned} A_g^{(n)} &= \partial_{\tilde{\mu}_g}^n\log(Z_g)|_{(\tilde{\mu}_g=0)}, \\ A_f^{(n)} &= \partial_{\tilde{\mu}_f}^n\log(Z_f)|_{(\tilde{\mu}_f=0)}. \end{aligned} \quad (12)$$

The explicit forms of A^n up to $n = 3$ are listed in the Appendix.

A. Explicit evaluation of the chemical potential

Before we discuss the solution of Eq. (10) and Eq. (11), it is instructive to evaluate $\mu_{g,f}$ with just the linear and quadratic terms for the sake of comparison. In the linear order, the

solutions read

$$\tilde{\mu}_g = \frac{8\pi^2}{45\left(A_g^{(1)}\right)}\left[A(\alpha_s) + B(\alpha_s)\ln\frac{\bar{\mu}_{\rm MS}\beta}{2\pi}\right], \quad (13)$$

$$\tilde{\mu}_f = \frac{8\pi^4}{45\left(A_f^{(1)}\right)}\left[C(\alpha_s) + D(\alpha_s)\ln\frac{\bar{\mu}_{\rm MS}\beta}{2\pi}\right], \quad (14)$$

whereas, in the next to the leading order, the solution has the form

$$\tilde{\mu}_g = -\frac{A_g^{(1)}}{A_g^{(2)}} \pm \sqrt{\left[\left(\frac{A_g^{(1)}}{A_g^{(2)}}\right)^2 + C_g\right]}, \quad (15)$$

$$\tilde{\mu}_f = -\frac{A_f^{(1)}}{A_f^{(2)}} \pm \sqrt{\left[\left(\frac{A_f^{(1)}}{A_f^{(2)}}\right)^2 + C_f\right]}, \quad (16)$$

where $C_g = 2\Delta P_g \beta V/A_g^{(2)}$ and $C_f = 2\Delta P_f \beta V/A_f^{(2)}$. Finally, the exact solutions can be obtained by using well-known algebraic techniques. Since the explicit algebraic solutions do not have an illuminating form, we show the solutions graphically instead in the next section.

The distribution functions for the gluons and the quarks get determined, in terms of the chemical potentials, through

$$\langle n_g\rangle_p = \frac{\exp(-\beta\epsilon_p + \tilde{\mu}_g)}{1-\exp(-\beta\epsilon_p+\tilde{\mu}_g)},$$
$$\langle n_f\rangle_p = \frac{\exp(-\beta\epsilon_p + \tilde{\mu}_f)}{1+\exp(-\beta\epsilon_p+\tilde{\mu}_f)}. \quad (17)$$

The extraction of the distribution functions is, nevertheless, incomplete because the EOS—and hence the chemical potentials—depend on the renormalization scale. However, the physical observables should be scale independent. We circumvent the problem by trading off the dependence on $\bar{\mu}_{\rm MS}$ to a dependence on the critical temperature T_c. To that end, we exploit the temperature dependence of the coupling constant $\alpha_s(T)$ [33][1] and of the renormalization scale:

$$\bar{\mu}_{\rm MS}(T) = 4\pi T\exp[-(\gamma_E + 1/22)],$$
$$\alpha_s(T) = \frac{1}{8\pi b_0\log(T/\lambda_T)} = \alpha_s(\mu^2)|_{\mu=\bar{\mu}_{\rm MS}(T)}, \quad (18)$$
$$\lambda_T = \frac{\exp(\gamma_E+1/22)}{4\pi}\lambda_{\rm MS},$$

where $b_0 = 33 - 2N_f/12\pi$ and $\lambda_{MS} = 1.14T_c$. With this step, the distribution functions get determined completely and are obtained as functions of T/T_c.

[1]The expression for the QCD running coupling constant displayed in Eq. (18) is allowed in the region where the weak perturbative techniques are valid. Because the weak coupling techniques give convergent results for more than $2T_c$, where T_c is the QCD transition temperature and a free parameter here, in this region, we can consider the asymptotic limit of the running coupling constant. Employing this, we shall see that the hot QCD EOS relative to the ideal EOS and effective chemical potentials scales with T/T_c.

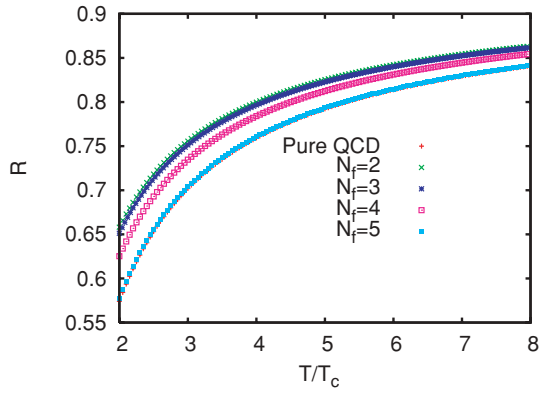

FIG. 1. (Color online) Behavior of R with temperature for EOS1.

We note that the results presented in the following, being valid for $T > 2T_c$, need to be supplemented by a similar analysis for equations of state that are valid for $T \sim T_c$. Such an analysis does indeed exist, along the lines of that presented by Allton *et al.* [32], who have considered the lattice EOS. They do not determine the Debye mass but focus on the impact of the EOS on the flow parameters in heavy ion collisions.

Although EOS1 and EOS2 have been computed within the framework of weak coupling technique they give convergent results for temperature ranges that are higher than $5T_c$. We shall see in the next section that these equations of state are far away from their ideal behavior up to the extent that they can be utilized to make definite predictions for QGP.

B. Hot QCD EOS versus ideal EOS

As a warm up, we compare EOS1 and EOS2 with the ideal EOS by plotting the ratio $R \equiv \frac{P}{P_q^I + P_g^I}$, as functions of temperature, in Figs. 1 and 2.

The most striking feature that we see is the large sensitivity to the inclusion of the $g^6\ln(\frac{1}{g})$ contributions. It is most pronounced in the behavior of pure QCD, where major qualitative and quantitative differences appear: (i) For EOS1, R increases with T, in contrast to EOS2, where it decreases from above, approaching the same asymptotic value for large T. (ii) Interestingly, the nonperturbative (and higher order)

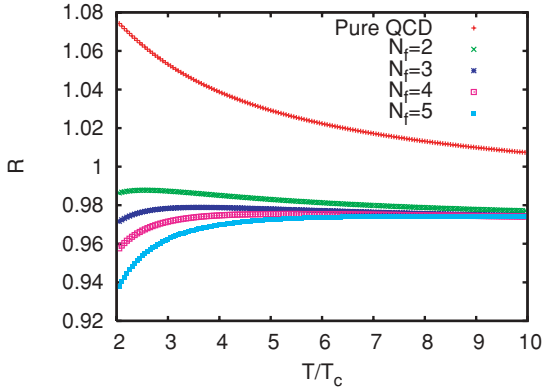

FIG. 2. (Color online) Behavior of R with temperature for EOS2.

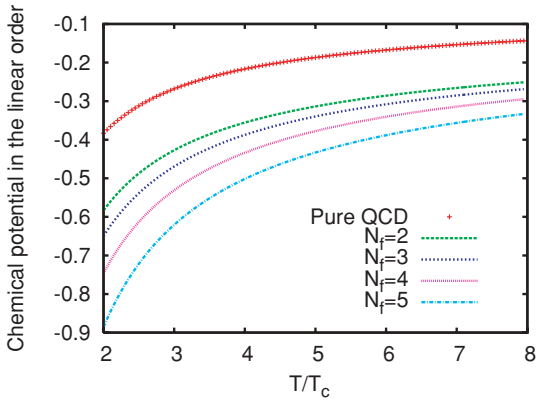

FIG. 3. (Color online) Effective chemical potentials at the linear order for EOS1.

corrections makes the system less nonideal. Indeed, EOS1 yields values of R that are 10%–45% away from the ideal value 1, in contrast to EOS2 (see Fig. 2), for which R is only 2%–8% away from the ideal value. Incidentally, this observation implies that the expansion in Eq. (8) works better for EOS2 than for EOS1. This will be reflected later in the behavior of effective chemical potentials with temperature. We shall further see that smaller the value of $|\tilde{\mu}_{g,f}|$ better will be the approximation.

C. The chemical potentials

The variation of the effective chemical potentials with renormalization scale at a fixed temperature has already been studied in Ref. [14]. We prefer to recast it into a dependence of $\tilde{\mu}_{g,f}$ on $\frac{T}{T_c}$ (see the previous section) since it is more relevant to the study of QGP in heavy ion collisions. This is shown in Figs. 3–8, where the contributions coming from linear, quadratic, and cubic approximations in the Taylor series [Eq. (8)] are individually displayed, for both EOS1 and EOS2. These figures exhibit, in essence, all the interaction effects.

A number of features emerge from examining Figs. 3–8. Consider EOS1 first. Here, the linear approximation does reasonably well for pure QCD, but it fails badly in the quark

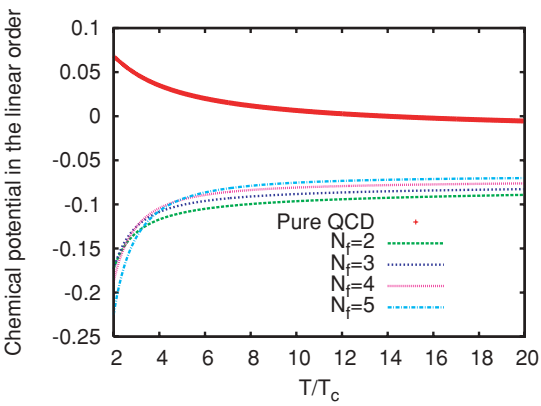

FIG. 4. (Color online) Effective chemical potentials at the linear order for EOS2.

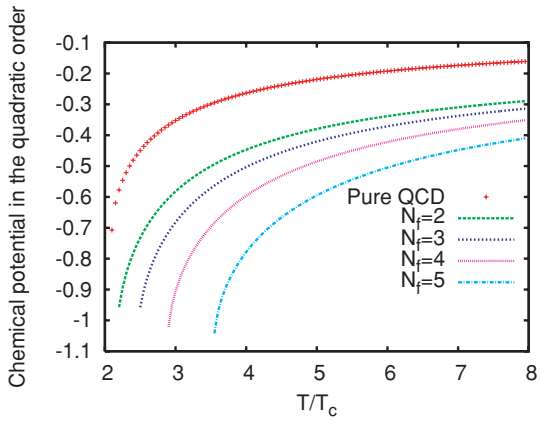

FIG. 5. (Color online) Effective chemical potentials at the quadratic order for EOS1.

sector. The chemical potential is negative in both sectors and approaches the ideal value asymptotically from below. In contrast, EOS2 leads to a different behavior: $\tilde{\mu}_g$ starts with a small positive value at $T \sim 2T_c$ and stays essentially constant until $T \sim 13T_c$, when it switches sign to acquire a small negative value. Since the magnitude remains less than 0.1 throughout, the deviation from the ideal behavior is minimal. The quark chemical potential $\tilde{\mu}_f$ remains negative (with a maximum magnitude $\sim$0.25 at $T = 2T_c$), which is about a one-quarter the corresponding value from EOS1. The interaction effects get manifestly stronger as we increase the number of flavors.

It is significant that the ideal value is not reached even at $T \sim 10T_c$, which indicates that the phase remains interacting. We also note that our method of extracting the chemical potential works more efficiently for EOS2, as indicated by small corrections from higher order terms to the linear estimate.

III. THE DEBYE MASS AND SCREENING LENGTH

The extraction of the equilibrium distribution functions affords a determination of the Debye mass m_D, via the

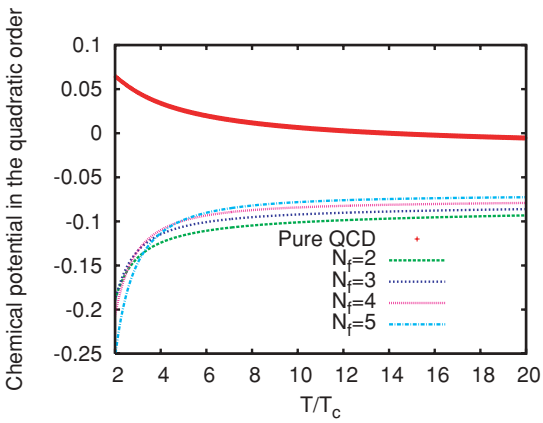

FIG. 6. (Color online) Effective chemical potentials at the quadratic order for EOS2.

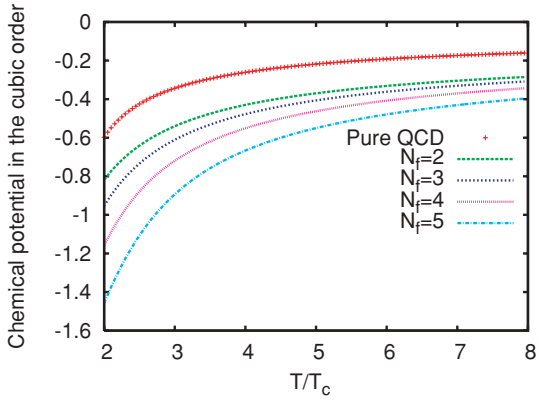

FIG. 7. (Color online) Effective chemical potentials at the cubic order for EOS1.

semiclassical transport theory [28]. The Debye mass controls the number of bound states in heavy $q\bar{q}$ systems, yields the extent of J/Ψ suppression in heavy ion collisions [38], provided that we have a reliable estimate of the temperature of the plasma. Even otherwise, the qualitative significance of the Debye mass cannot be overestimated because the deconfined phase remains strongly interacting even at large T.

The determination of m_D is straightforward if we employ the classical transport theory [28]. It is simply given by

$$M_{g,f}^2 = g'^2 C_{g,f} \int \frac{d}{dp_0} \langle n_{g,f} \rangle d^3 p. \tag{19}$$

This expression has to be used cautiously, though. The coupling constant g' in Eq. (19) has a phenomenological character, and it should not be confused with the fundamental constant g appearing in the EOS. Keeping this in mind, we recall that if the plasma were to be comprised of ideal massless partons, the Debye mass would be given by

$$M_{\rm id}^2 = M_{g,\rm id}^2 + M_{f,\rm id}^2 \equiv \frac{(N + N_f/2)}{3} g'^2 \beta^{-2}. \tag{20}$$

The hot QCD equations of state modify this expression. It is easy to see, from Eqs. (19) and (20), that the new Debye masses, scaled with respect to their respective ideal values, get

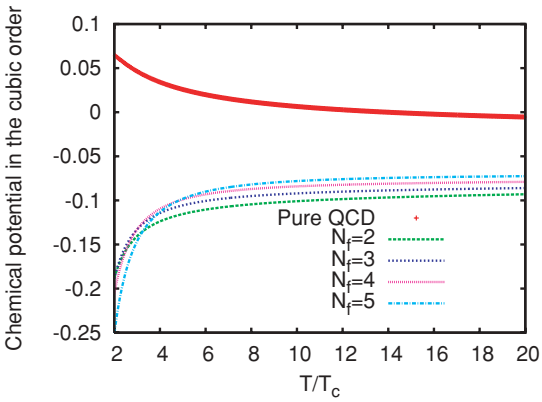

FIG. 8. (Color online) Effective chemical potentials at the cubic order for EOS2.

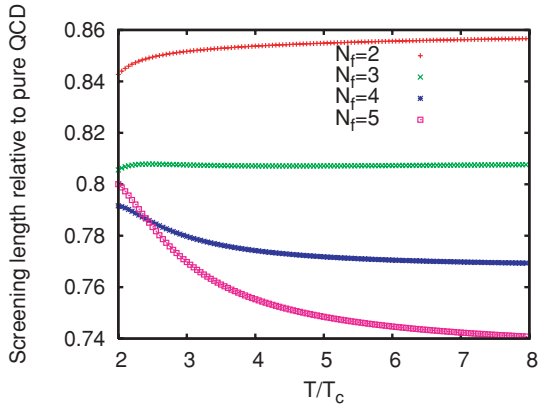

FIG. 9. (Color online) The relative Debye screening length $\mathcal{R}_{h/g}$ for EOS1 as a function of temperature. Note that it is $\mathcal{R}_{h/g} \geqslant 0.7$.

determined in terms of the standard PolyLog functions[2] by

$$\frac{M_{g,\rm hot}^2}{M_{g,\rm id}^2} = \frac{6}{\pi^2} \text{PolyLog}[2, \exp(\tilde{\mu}_g)] \equiv F_1(\tilde{\mu}_g),$$
$$\frac{M_{f,\rm hot}^2}{M_{f,\rm id}^2} = -\frac{12}{\pi^2} \text{PolyLog}[2, -\exp(\tilde{\mu}_f)] \equiv F_2(\tilde{\mu}_f). \tag{21}$$

Consequently, the expression for the total relative mass is obtained as

$$\frac{M_{\rm hot}^2}{M_{\rm id}^2} = \frac{\left[\frac{N}{3} F_1(\tilde{\mu}_g) + \frac{N_f}{6} F_2(\tilde{\mu}_f)\right]}{(N/3 + N_f/6)}. \tag{22}$$

It is, however, more convenient to plot the inverse Debye mass (i.e, the screening length) as a function of T/T_c.

A. Relative screening lengths

We first establish the notation. Let λ_h denote the screening length generated by the hot EOS. Let $\lambda_{\rm id}$ be the screening

[2]The function PolyLog$[2, z]$ is defined by the series PolyLog$[2, z] = \sum_{k=1}^{\infty} \frac{z^k}{k^2}$, with a radius of convergence given by $|z| < 1$.

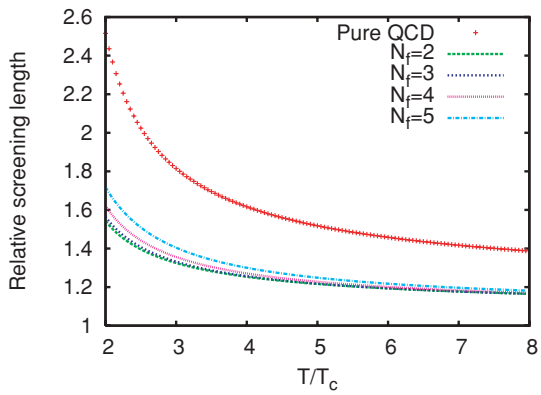

FIG. 10. (Color online) The relative screening length $\mathcal{R}_{h/\rm id}$ for EOS1 as a function of temperature.

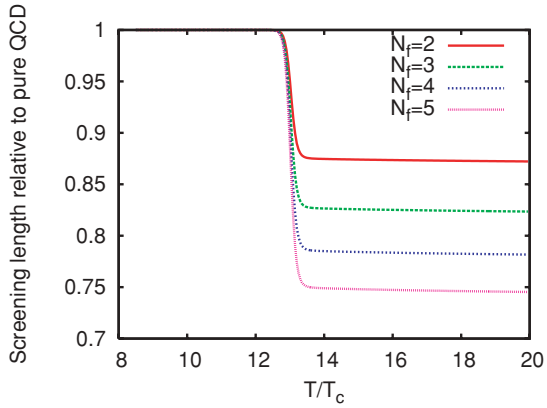

FIG. 11. (Color online) The relative Debye screening length $\mathcal{R}_{h/g}$ for EOS2 as a function of temperature. Note that $\mathcal{R}_{h/g}$ stays at 1 all the way up to $13T_c$.

length of an ideal QGP. It is convenient to consider also the contribution coming from the pure QCD sector, whose screening lengths we denote by λ_h^g and $\lambda_{\rm id}^g$, respectively.

The behavior of the screening lengths is shown in Figs. 9–12. As in the case of the chemical potentials, the dependence on the order of perturbation is striking here as well. For EOS1, where the contributions up to $O(g^5)$ are included, the screening lengths in the full QCD as well as pure QCD remain nonzero. The dominant contribution is from the gluonic sector, which dominates over the quark sector, as may be seen in Fig. 9 where we plot the ratio $\mathcal{R}_{h/g} = \lambda_h/\lambda_h^g$, which is in excess of 0.7 throughout. Note, however, that the relative dominance gets weaker as we increase the number of flavors. Figure 10 shows the variation of the ratio $\mathcal{R}_{h/\rm id} = \lambda_h/\lambda_{\rm id}$ as a function of temperature. Interestingly, the interaction is seen to weaken the screening, and so does an increase in the number of flavors.

These results are in sharp contrast with the case of EOS2, which we recall has nonperturbative $O[g^6 \ln(1/g)]$ contributions. These are shown in Figs. 11 and 12. It is clear from Fig. 11 that the contribution from the pure gluonic sector saturates the contribution to the screening all the way up to temperatures $T \sim 13T_c$ and drops sharply thereafter. This feature is reinforced by Fig. 12, where the ratio $\mathcal{R}_{h/\rm id}$

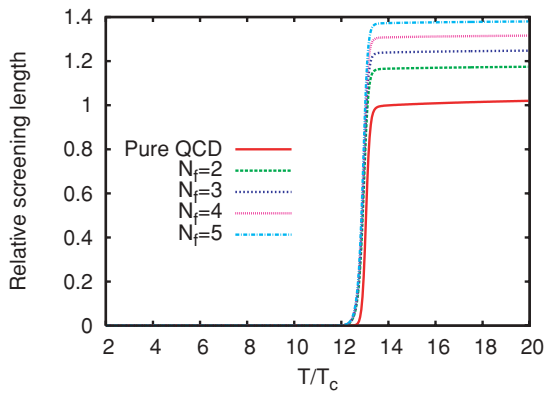

FIG. 12. (Color online) The relative screening length $\mathcal{R}_{h/\rm id}$ for EOS2 as a function of temperature.

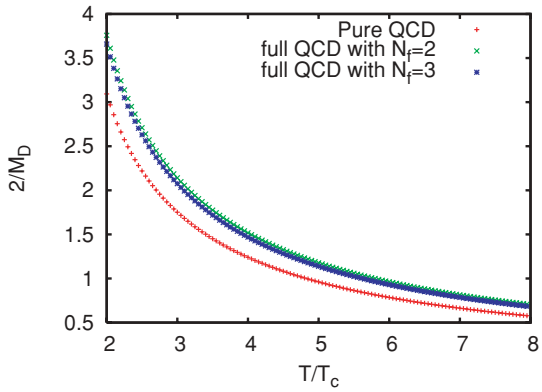

FIG. 13. (Color online) Behavior of $2/M_D$ with T/T_c for $g' = 0.3$ for EOS1. Note that $2/M_D$ is measured in femtometers.

stays at zero between $2T_c$ and $12T_c$–$13T_c$. It is of a purely academic interest that the screening length should become nonzero beyond $12T_c$.

It appears that the perfect screening is indeed the strongest prediction of EOS2 and must be most easily tested in heavy ion collisions, where temperatures up to $3T_c$ are expected at LHC. This is in sharp contrast with the assumptions of a near ideal behavior and also some theoretical analyses, which in fact propose an enhanced production of J/Ψ at LHC energies [34]. We, therefore, attempt to compare these predictions with the lattice results in the following.

B. Comparison with the lattice results

In this section, we compare our results on screening length of EOS1 and EOS2 with the lattice results. Lattice computations extract the screening lengths from the quark-antiquark free energies. To be concrete, we make the comparison with three distinct values of the coupling constant, $g' = 0.3$, 0.5, and 0.8.

Further, we consider three cases: (i) pure QCD, (ii) $N_F = 2$, and (iii) $N_F = 3$. To facilitate a proper comparison, we take the respective transition temperatures to be $T_c = 270$, 203, and 195 MeV, as given by lattice computations. The comparison is shown only with EOS1 since EOS2 predicts absolute screening

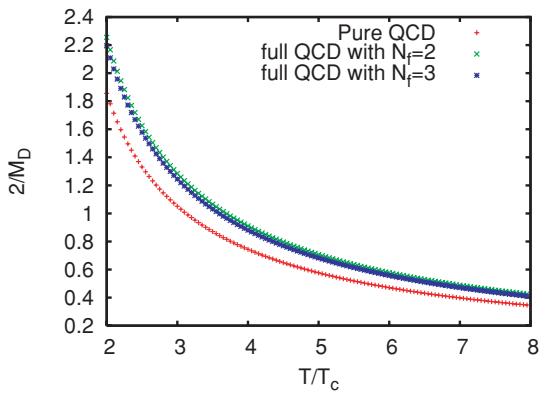

FIG. 14. (Color online) Behavior of $2/M_D$ with T/T_c for $g' = 0.5$ for EOS1. Note that $2/M_D$ is measured in femtometers.

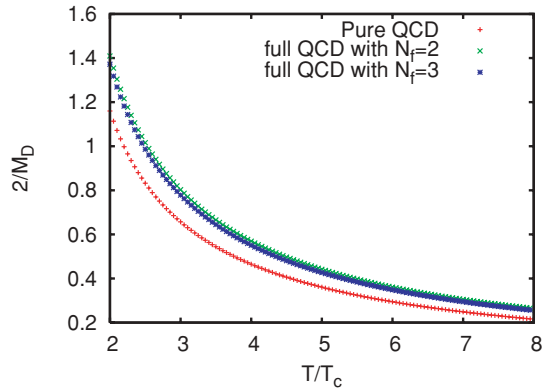

FIG. 15. (Color online) Behavior of $2/M_D$ with T/T_c for $g' = 0.8$ for EOS1. Note that $2/M_D$ is measured in femtometers.

in the range $2T_c < T < 12T_c$ in which we are interested. The results are shown in Figs. 13–15. As observed, the screening weakens with increasing g'; moreover, the screening weakens with the increase in the number of flavors as well. For an explicit comparison, we consider the results reported by Kaczmarek and Zantow [35], who determine the screening length by identifying it essentially with the first moment of the $q\bar{q}$ free energy. Their results are displayed in Fig. 2 of Ref. [35], to which we refer henceforth. Interestingly, the same qualitative features are exhibited for EOS1 and the lattice results, in both aspects (i.e., the dependence on the coupling constant as well as on the number of flavors). However, the agreement fails to get quantitative. The lattice results predict screening lengths that are smaller in value, except for $N_F = 3$, than the EOS1 results. Indeed, the lattice screening length is $\sim$0.7 fm in the vicinity of T_c, and it drops to $\sim$0.4 fm close to $2T_c$. It is evident from Figs. 13–15 that the results of EOS1 are 3 to 10 times higher in value. Any better agreement with a further increase in the value of g' is ruled out since $g' \leqslant 1$ necessarily.

IV. CONCLUSIONS AND OUTLOOK

In conclusion, we have extracted the distribution functions for gluons and quarks from two equations of state, in terms of effective chemical potentials for the partons. The chemical potentials are shown to be highly sensitive to the inclusion of $O[g^6 \ln(1/g)]$ contributions, as exhibited most vividly by the screening length. Surprisingly, EOS2, which has interactions up to $O[g^6 \ln(1/g)]$, shows less nonideal behavior compared to EOS1 [which has contributions up to $O(g^5)$]. Equally strikingly, the plasma corresponding to EOS2 is predominantly gluonic, in the sense that the Debye mass from the gluonic sector diverges in the range $2T_c \leqslant T \leqslant 12T_c$. This result contrasts with that of the less precise EOS1, where the gluonic contribution is not that overwhelming.

To place our analysis in perspective, we note that our analysis is based on but two equations of state, neither of which has full nonperturbtive contributions. Nevertheless, it may not be without merit: EOS2, for instance, makes rather strong predictions that may be tested and EOS1 is seen to be in qualitative agreement with the lattice results. Indeed, the work does provide a platform to study quantitatively the import of the EOS to heavy ion collisions in a quantitative manner. Experiments at LHC may be able to probe these equations of state since a temperature in the range $T \sim 2T_c$–$3T_c$ is expected to be achieved there. More importantly, the method developed here can be easily employed to study equations of state that are more precise (from lattice computations) or more general (from the inclusion of baryonic chemical potentials). To be sure, an incisive analysis is possible only after studying other quantities such as the viscosity, its anomalous component [36,37], the viscosity to entropy ratio, and the specific heat. Finally, the insertion of the appropriate equilibrium distribution functions in the semiclassical transport equations allow for studying (i) the production and the equilibration rates for the QGP in heavy ion collisions [24–26] and (ii) the color response functions [39], of which the Debye mass is but one limiting parameter. These topics will be taken up in subsequent publications and will be investigated separately.

ACKNOWLEDGMENTS

We thank D. D. B. Rao for assistance with numerical work. Two of us, VC and RK, acknowledge CSIR (India) for financial support.

APPENDIX

We use the following standard integrals while extracting effective chemical potential:

$$\int_0^\infty p^2 \frac{\exp(-p)}{[1-\exp(-p)]^3} dp = 2\left\{1 + \sum_{n=1}^{\infty}\left[\frac{1}{(n+1)^3}\prod_{k=1}^{n}\frac{3+k-1}{k!}\right]\right\},$$

$$\int_0^\infty p^2 \frac{\exp(2p)}{[1+\exp(p)]^3} dp = \frac{\pi^2}{12} + \log(2), \tag{A1}$$

$$\int_0^\infty p^2 \frac{\exp(p)}{[1-z\exp(p)]^2} dp = \frac{\mathrm{PolyLog}[2,z]}{z},$$

$$\int_0^\infty p^2 \frac{\exp(p)}{[1+z\exp(p)]^2} dp = -\frac{\mathrm{PolyLog}[2,-z]}{z}. \tag{A2}$$

The coefficients in the perturbative expansion of $\log(Z_g)$ and $\log(Z_f)$ are as follows:

$$A_g^{(1)} = \frac{V}{2\pi^2 g_b} 2\zeta(3),$$

$$A_f^{(1)} = \frac{V}{2\pi^2 g_f} \frac{3}{2}\zeta(3),$$

$$A_g^{(2)} = \frac{V}{2\pi^2 g_b} \frac{\pi^3}{3},$$

$$A_f^{(2)} = \frac{V}{2\pi^2 g_f}\frac{\pi^3}{6},$$

$$A_f^{(3)} = \frac{V}{2\pi^2 g_f} 2\log(2),$$

$$A_g^{(3)} = \frac{V}{2\pi^2 g_b} \times \left\{ 4\left[1 + \sum_{n=1}^{\infty} \left(\frac{1}{(n+1)^3} \prod_{k=1}^{n} \frac{3+k-1}{k!} \right) \right] - \frac{\pi^2}{3} \right\}, \tag{A3}$$

where $g_b = 8 \times 2$ and $g_f = 6N_f$ are the degeneracy factors for gluons and quarks, respectively.

[1] STAR Collaboration, Nucl. Phys. **A757**, 102 (2005).
[2] PHENIX Collaboration, Nucl. Phys. **A757**, 184 (2005).
[3] PHOBOS Collaboration, Nucl. Phys. **A757**, 28 (2005).
[4] BRAHMS Collaboration, Nucl. Phys. **A757**, 01 (2005).
[5] K. Adcox *et al*., Phys. Rev. Lett. **88**, 022301 (2002); C. Adler *et al*., *ibid*. **89**, 202301 (2002); S. S. Adler *et al*., *ibid*. **91**, 072301 (2003); J. Adams *et al*., *ibid*. **91**, 172302 (2003).
[6] M. J Tannenbaum, Rep. Prog. Phys. **69**, 2005 (2006).
[7] D. Teaney, Phys. Rev. C **68**, 034913 (2003).
[8] R. Baier and P. Romatschke, arXiv: nucl-th/0610108.
[9] H.-J. Drescher, A. Dumitru, C. Gombeaud, and J.-Y. Ollitrault, Phys. Rev. C **76**, 024905 (2007).
[10] P. K. Kovtun, D. T. Son, and A. O. Starinets, Phys. Rev. Lett. **94**, 111601 (2005).
[11] G. Boyd, J. Engels, F. Karsch, E. Laermann, C. Legeland, M. Lütgemeier, and B. Petersson, Nucl. Phys. **B469**, 419 (1996); Phys. Rev. Lett. **75**, 4169 (1995); R. Gavai, Pramana **67**, 885 (2006); F. Karsch, Nucl. Phys. **A698**, 199 (2002); Y. Aoki, Z. Fodor, S. D. Katz, K. K. Szabo, U. Wuppertal, and U. Eotvos, J. High Energy Phys. 01 (2006) 089.
[12] E. V. Shuryak, Nucl. Phys. **A774**, 387 (2006).
[13] P. Arnold and C. Zhai, Phys. Rev. D **50**, 7603 (1994); **51**, 1906 (1995).
[14] C. Zhai and B. Kastening, Phys. Rev. D **52**, 7232 (1995).
[15] K. Kajantie, M. Laine, K. Rummukainen, and Y. Schroder, Phys. Rev. D **67**, 105008 (2003).
[16] K. Kajantie, M. Laine, K. Rummukainen, and Y. Schroder, Phys. Rev. Lett. **86**, 10 (2001).
[17] A. Ipp, K. Kajantie, A. Rebhan, and A. Vuorinen, Phys. Rev. D **74**, 045016 (2006).
[18] J. P. Blaizot, E. Iancu, and A. Rebhan, Phys. Rev. D **63**, 065003 (2001).
[19] J. P. Blaizot, E. Iancu, and A. Rebhan, Phys. Lett. **B523**, 143 (2001).
[20] A. Rebhan, talk given at the 4th Budapest Winter School on Heavy Ion Physics, 1–3 December 2004, arXiv:hep-ph/0504023 and references therein.
[21] A. Rebhan, J. High Energy Phys. 06 (2003) 032.
[22] U. Kraemmer and A. Rebhan, Rep. Prog. Phys. **67**, 351 (2004).
[23] J.-P. Blaizot, E. Iancu, and A. Rebhan, Phys. Rev. Lett. **83**, 2906 (1999).
[24] G. C. Nayak and V. Ravishankar, Phys. Rev. C **58**, 356 (1998); Phys. Rev. D **55**, 6877 (1997).
[25] R. S. Bhalerao and V. Ravishankar, Phys. Lett. **B409**, 38 (1997).
[26] A. Jain and V. Ravishankar, Phys. Rev. Lett. **91**, 112301 (2003).
[27] P. F. Kelly, Q. Liu, C. Lucchesi, and C. Manuel, Phys. Rev. Lett. **72**, 3461 (1994).
[28] P. F. Kelly, Q. Liu, C. Lucchesi, and C. Manuel, Phys. Rev. D **50**, 4209 (1994).
[29] J.-P. Blaizot and E. Iancu, Phys. Rev. Lett. **70**, 3376 (1993).
[30] A. Vuorinen, Phys. Rev. D **68**, 054017 (2003).
[31] A. Peshier *et al*., Phys. Lett. **B337**, 235 (1994); A. Peshier, B. Kampfer, O. P. Pavlenko, and G. Soff, Phys. Rev. D **54**, 2399 (1996); A. Peshier, B. Kampfer, and G. Soff, Phys. Rev. C **61**, 045203 (2000); Phys. Rev. D **66**, 094003 (2002).
[32] C. R. Allton, S. Ejiri, S. J. Hands, O. Kaczmarek, F. Karsch, E. Laermann, and C. Schmidt, Phys. Rev. D **68**, 014507 (2003); C. R. Allton, M. Döring, S. Ejiri, S. J. Hands, O. Kaczmarek, F. Karsch, E. Laermann, and K. Redlich, *ibid*. **71**, 054508 (2005); For a very recent work, see M. Bluhm, B. Kämpher, R. Schulze, D. Seipt, and U. Heinz, arXiv:0705.0397.
[33] S. Haung and M. Lissia, Nucl. Phys. **B438**, 54 (1995).
[34] G. Aarts, C. Allton, M. B. Oktay, M. Peardon, and J.-I. Skullerud, arXiv:0705.2198[hep-lat].
[35] O. Kaczmarek and F. Zantow, PoS LAT2005, 177 (2005).
[36] P. Arnold, G. D. Moore, and L. G. Yaffe, J. High Energy Phys. 01 (2000) 011.
[37] M. Asakawa, S. A. Bass, and B. Müller, Phys. Rev. Lett. **96**, 252301 (2006); Prog. Theor. Phys. **116**, 725 (2007); A. Majumdar and B. Müller, hep-ph/0703082.
[38] T. Matsui and H. Satz, Phys. Lett. **B178**, 416 (1986).
[39] Akhilesh Ranjan and V. Ravishankar, arXiv:0707.3697 [nucl-th].